Bull. Chem. Soc. Ethiop. **2022**, 36(2), 373-385.
© 2022 Chemical Society of Ethiopia and The Authors
DOI: https://dx.doi.org/10.4314/bcse.v36i2.11

ISSN 1011-3924
Printed in Ethiopia
Online ISSN 1726-801X

FOUR NEW TIN(II), URANYL(II), VANADYL(II), AND ZIRCONYL(II) ALLOXAN BIOMOLECULE COMPLEXES: SYNTHESIS, SPECTROSCOPIC AND THERMAL CHARACTERIZATIONS

Amnah Mohammed Alsuhaibani[1], Abdel Majid A. Adam[2] and Moamen S. Refat[2*]

[1]Department of Physical Sport Science, College of Education, Princess Nourah bint Abdulrahman University, P.O. Box 84428, Riyadh 11671, Saudi Arabia
[2]Department of Chemistry, College of Science, Taif University, P.O. Box 11099, Taif 21944, Saudi Arabia

(Received March 29, 2022; Revised April 15, 2022; Accepted April 18, 2022)

ABSTRACT. The alloxan as a biomolecule ligand has been utilized to synthesize thermodynamically and kinetically stabilized four new tin(II), uranyl(II), vanadyl(II), and zirconyl(II) complexes. In the complexes, tin(II) ion present is in tetrahedral arrangement, zirconyl and vanadyl(II) ions present are in square pyramid feature but uranyl(II) ion present is in octahedral arrangement and all are coordinated by two bidentate alloxan ligand in complexes. The synthesized alloxan ligand coordinate with central metal(II) ion through oxygen in position C_2=O and the nitrogen in position N_1 developing a 4-membered chelate ring. Synthesized Sn(II), UO_2(II), VO(II), and ZrO(II) complexes via bidentate ligand have been accurately described by various spectroscopic techniques like elemental analysis (C, H, N, metal), conductivity measurements, FT-IR, UV-Vis, ^{1}H-NMR, and TGA. The kinetic thermodynamic parameters such as: E^*, ΔH^*, ΔS^* and ΔG^* were calculated using Coats and Redfern and Horowitz and Metzger equations.

KEY WORDS: Alloxan, Metal ions, Spectroscopy, Ligand, Coordination, Thermogravimetry

INTRODUCTION

Brugnatelli [1] was the first scientist who was isolated "Alloxan", as a pyrimidine derivative and subsequently found that this compound possesses a biological and antitumor properties [2]. Alloxan, ($C_4H_4N_2O_5$) is broadly utilized in test diabetes ponders, since this specialist devastates pancreatic islet beta cells with selectivity [3-5]. The ponder of the instrument of activity of a normal glycolytic specialist shows up to be of incredible significance for illustrating the cause of insulin-dependent diabetes mellitus. Alloxan is known to restrain proinsulin blend in pancreatic islets [6]. Ushigata and others were proposed that alloxan initiated DNA strand breaks to fortify poly(ADP-ribose) nuclear, in this way draining the intracellular NAD level and hindering proinsulin blend [7,8]. Undoubtedly, islet DNA strand breaks were watched in vivo by organization of alloxan to rats [9]. Alloxan can impact the calcium, zinc, and phosphorous digestion system in living life forms to extend blood sugar. Hence, it can be utilized in exploratory ponders of diabetes [10]. Additionally, alloxan is show in living organisms, and could be an item of the breakdown of uric acid [11]. The tall natural movement of alloxan decides the incredible intrigued of researchers with its complex intuitive. Hence, Co(II), Ni(II), and Cu(II) complexes with alloxan and $ML_2.5H_2O$ were separated from soluble watery arrangements [12]; manganese(II) alloxan was gotten by evaporating an acidified solvent at room temperature [13]. As takes after from the spectroscopic information, cerium(III) shapes with alloxan the dissolvable ML_2 complex [14]. It is known that transition metal salts respond with alloxan arrangements to donate colored complexes: orange-yellow or red for Cd(II), Mg(II), Cu(II), Zn(II), Co(II), Ni(II), dull blue (within the nearness of alkali) for iron(II) [15]. The structures and properties of Pb(II), Hg(I), Hg(II), and Ag(I) alloxan have been examined in detail [15-18].

---

*Corresponding author. E-mail: moamen@tu.edu.sa

Kovalchukova *et al.* were considered Fe(III) and Co(III) complexes with alloxan [19, 20]. The synthesis of Co(II), Ni(II), and Pd(II) alloxan have moreover been detailed [21]. The think about of arrangement complexes of d and f block metals with alloxan was carried out by Shebaldina *et al.* [22]. Alloxan is one of the modified serrated bonds that gives a metal particle in more than one comparable coordination location (Figure 1). Fundamentally, there's continuously a conceivable improvement in joins with modified serrations in which the metal is exchanged from one location to another. This could be either an intramolecular or intramolecular prepare. The modification response is dynamically controlled by the actuation vitality and entropy that the metal experiences over the course of the response. The free energy contrast is zero, on the off chance that the coordination locales are comparable [24, 25]. It is known that hydrated alloxan can exist in different filler shapes (Figure 1) [23, 26]:

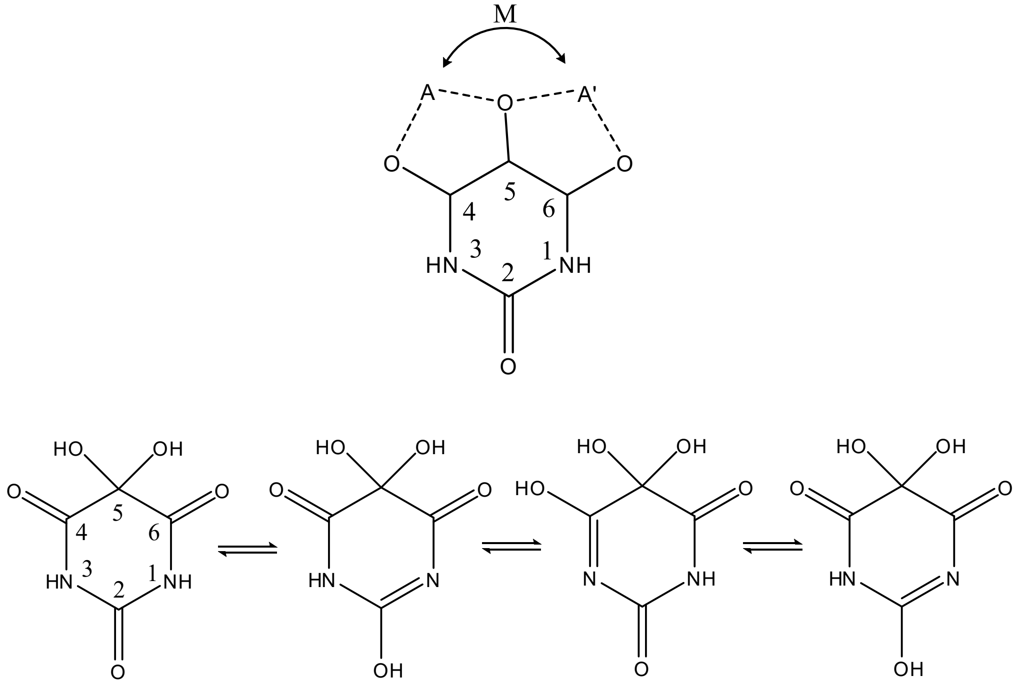

lactam monoenol I monoenol II dienol

Figure 1. The structure possibilities of alloxan molecule.

The calculated dissolution temperatures (ΔH) demonstrated that among all the displayed shapes, the monoenol II shape is most steady within the gas stage (ΔH = 62.71 eV). The stability of the monoenol I, dienol and lactam shapes is to some degree lower (ΔH = 62.44, 62.64 and 62.65 eV, individually). Agreeing to the X-ray diffraction information [27-29], the alloxan crystalline particle exists within the shape of a lactam (tri-oxo). In any case, the near intermolecular interaction energies of the over subordinates (4.86, 4.27, 4.53, 5.22 eV) make it conceivable to propose that in arrangements a few shapes exist at the same time, and they can be stabilized amid complexings. A writing overview of alloxan complexes has appeared that alloxans can arrange through a few sorts of structures (Figure 2).

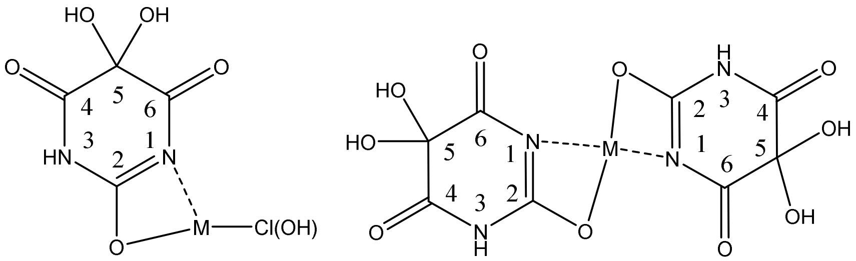

Type 1: Ref. [23]

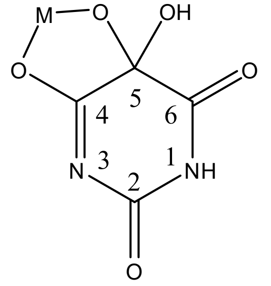

Type 2: Ref. [23]

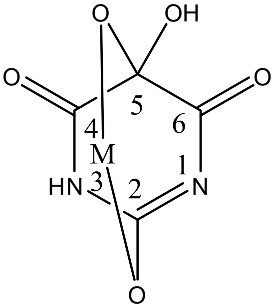

Type 3: Ref. [23]

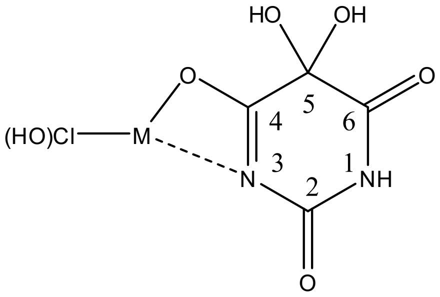

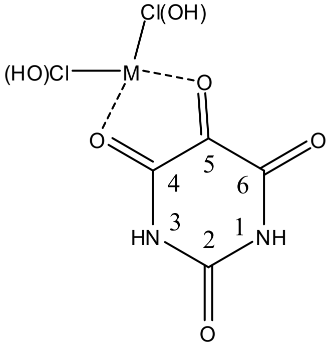

Type 4: Ref. [19, 29]

Type 5: Ref. [30]

Figure 2. The different coordination sites of alloxan molecule towards central metal ions.

This investigation was conducted to think about the response pathway between alloxan and different metal ions such as Sn(II), UO_2(II), VO(II), and ZrO(II). Solid products were characterized by spectrophotometry. The stability of the arranged alloxan complexes was inspected utilizing thermogravimetric examination and thermodynamic calculations.

EXPERIMENTAL

Materials and instrumentations

All chemicals and solvents utilized within the manufactured of the complexes were acquired from Merck (Darmstadt, Germany) and Sigma Aldrich (St Louis, Mo, USA) and utilized without assist purification unless something else famous. The carbon, hydrogen and nitrogen percentages were performed employing a Perkin-Elmer CHN 2400. The metal substance was found gravimetrically by changing over the compounds into their comparing oxides at 800 ºC under static air condition. Molar conductivities of naturally arranged 10^{-3} M DMSO arrangements were measured utilizing Jenway 4010 conductivity meter. FTIR spectra were checked utilizing Genesis II FTIR Spectrometer within the (4000–400 cm^{-1}) run with 40 scans in KBr discs. The UV–Vis spectra were decided within the DMSO dissolvable with concentration (10^{-3} M) for the alloxan and their complexes using Jenway 6405 Spectrophotometer with 1cm quartz cell, within the extend 800–200 nm. ^{1}H-NMR spectra were performed on Bruker Development 300 MHz equipment utilizing DMSO-d_6 as dissolvable and TMS as an internal reference. TGA and DTG curves were gotten on a Rigaku 8150 thermoanalyser under dynamic nitrogen air, at a heating rate of 5 deg min^{-1}.

Synthesis

I *- [Sn($C_4H_3N_2O_5$)$_2$].10H_2O ($C_8H_{26}N_4O_{20}Sn$) complex.* Alloxan monohydrate (0.32 g, 2 mmol) was dissolved in 25 mL methanol. This solution was included to 10 mL aqueous solution of $SnCl_2.2H_2O$ (0.226 g, 1.0 mmol) with persistent mixing for approximately 3 hours. The mixture was refluxed at 70 ºC. Ammonium hydroxide was included to alter pH at ~ 8. Instantly, the yellowish white precipitate was settled down and filtered off, washed a few times by least sums of hot methanol and dried under vacuo over anhydrous $CaCl_2$.

II *- [UO_2($C_4H_3N_2O_5$)$_2$].4H_2O ($C_8H_{14}N_4O_{16}U$) complex.* A comparative method as that depicted for complex **I** was carried out, by blending (0.32 g, 2 mmol) of alloxan monohydrate with $UO_2(NO_3)_2{\cdot}6H_2O$ (0.503 g, 1.0 mmol), the pH was balanced at ~ 8. The yellow powder precipitated was separated.

III *- [VO($C_4H_3N_2O_5$)$_2$].6H_2O ($C_8H_{18}N_4O_{17}V$) complex.* A dark green complex, $[VO(C_4H_3N_2O_5)_2].6H_2O$ was arranged during the reaction of (0.32 g, 2 mmol) alloxan monohydrate with (0.163 g, 1.0 mmol) of vanadium (IV) oxide sulfate hydrate by a strategy like that utilized for the arrangement of complex **I**, the pH was balanced at ~ 8.

IV *- [ZrO($C_4H_3N_2O_5$)$_2$].8H_2O ($C_8H_{22}N_4O_{19}Zr$) complex.* A watery solution of $ZrOCl_2.8H_2O$ (0.323 gm, 1.0 mmol) was mixed with alloxan monohydrate solution (0.32 g, 2.0 mmol) in methanol dissolvable. The mixture was permitted to remain at room temperature for around 3 h with proceeds mixing and after that refluxed on a hotplate at ~ 70 ºC for 2 h, the pH was balanced at ~ 8. The white creamy complex was filtered off, washed a few times with hot methanol, dried under vacuo over anhydrous $CaCl_2$.

RESULTS AND DISCUSSION

Microanalytical and physical study

All synthesized Sn(II), UO_2(II), VO(II), and ZrO(II) alloxan complexes are steady and colored compounds. These complexes were prepared in a yield (65-77%). All are insoluble in water, ethanol, methanol, and most of organic solvents but soluble in common organic solvents like

DMSO and DMF. The microanalytical and physical results of the gotten compounds are given in Table 1. The synthesized alloxan complexes have a higher melting point over >300 °C. The microanalytical investigation information of the complexes found that a 1:1 stoichiometry (metal: ligand) with molecular formulas $[Sn(C_4H_3N_2O_5)_2].10H_2O$, $[UO_2(C_4H_3N_2O_5)_2].4H_2O$, $[VO(C_4H_3N_2O_5)_2].6H_2O$, and $[ZrO(C_4H_3N_2O_5)_2].8H_2O$ (Figure 3). The alloxan complexes were characterized utilizing essential investigation that the observed and theoretical comes about are in near agreement with the proposed formulas.

Table 1. Microanalytical and physical data of the synthesized alloxan complexes.

Complex	Color	M.P/(°C)	Conductance/ ($ohm^{-1}.cm^2.mol^{-1}$)	Elements	%Calc.	%Found
Sn(II)	Yellowish white	>300	14	%C	15.57	15.49
				%H	4.25	4.19
				% N	9.08	9.02
				%Sn	19.24	19.20
UO_2(II)	Yellow	>300	16	%C	14.55	14.38
				%H	2.14	2.11
				% N	8.49	8.43
				%U	36.05	36.01
VO(II)	Dark green	>300	10	%C	19.48	19.42
				%H	3.68	3.63
				% N	11.36	11.32
				%V	10.33	10.31
ZrO(II)	White creamy	>300	18	%C	16.87	16.84
				%H	3.89	3.84
				% N	9.84	9.81
				%Zr	16.02	15.98

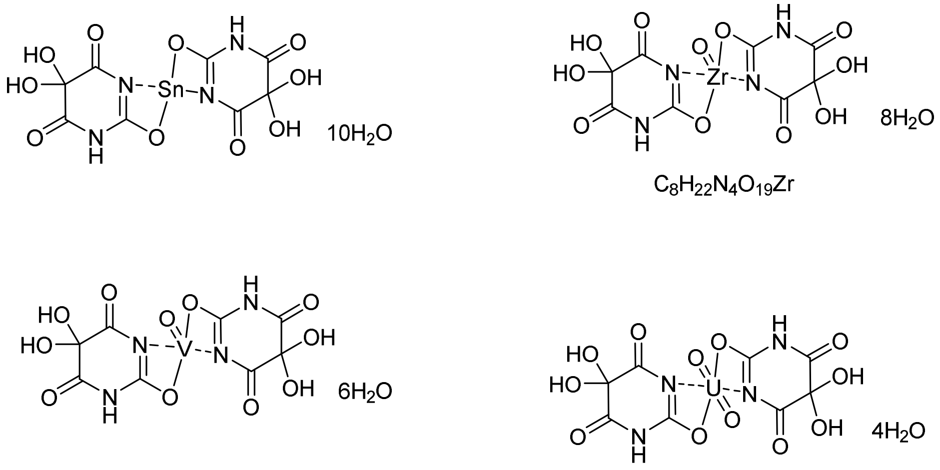

Figure 3. Speculated structures of Sn(II), UO(II), VO(II), and ZrO(II) alloxan complexes.

Conductivity estimations have regularly been utilized to explain the structure of metal chelates (coordination strategy) inside their solvency limits. They give a way to test the degree of ionization of complexes, the molecular ions a compound releases in arrangement in case the anions are exterior the coordination space), the higher the molar conductivity and vice versa [31]. Molar conductivity results of the Sn(II), UO_2(II), VO(II), and ZrO(II) alloxante complexes dissolved in DMSO solvent with concentration 10^{-3} M are found inside the run of 10–18 $ohm^{-1}.cm^2.mol^{-1}$ as a non-electrolytic behavior (Table 1). Agreeing, to the molar conductance information, it can be found that the anions are missing. These results are emphatically affirmed with the microchemical examination where ions are not identified by addition of appropriate reagent.

Infrared spectra

The distinguish infrared spectral bands of free alloxan molecule beside of the synthesized Sn(II), UO(II), VO(II), and ZrO(II) alloxante complexes are listed in Table 2 and the spectral curves are display in Figure 4. Regarding the FTIR assignments bands of the free alloxan, there are some intense bands in the regions 1764, 1737 and 1726 cm^{-1} attributed to the vibration motions of carbonyl groups. The band at 1764 cm^{-1} was assigned to the vibrations of the carbonyl group in the alloxan amide fragment (–NH–CO–NH–) and the bands at 1737 cm^{-1} and 1726 cm^{-1} can be assigned to vibrations of the ketone group in position 5 and the two ketone groups in positions 4 and 6, respectively [19, 20]. In the region of 3339–3044 cm^{-1}, there are broad intense bands attributed to overlapping vibrations of the NH and OH groups. In case of the spectra of the synthesized alloxanate complexes $[Sn(C_4H_3N_2O_5)_2].10H_2O$, $[UO_2(C_4H_3N_2O_5)_2].4H_2O$, $[VO(C_4H_3N_2O_5)_2].6H_2O$, and $[ZrO(C_4H_3N_2O_5)_2].8H_2O$, the band of the carbonyl groups in positions 4 and 6 which appear in the range (1727-1711 cm^{-1}) remain unchanged, while the bands at 1764 and 1737 cm^{-1} absent due to the formation of hydroxyl group, the metal chelating ring in these compounds involving the oxygen in position 2 and the nitrogen in position 1, as shown in Type 1 [23].

The bands appeared at 985 and 875 cm^{-1} assigned for υ_3 and υ_1 of dioxouranium [31-35]. The value of ν_3 is used to calculate the force constant (F) of O=U=O by the method of McGlynn and smith [32-35]: $(\nu_3)^2 = (1307)^2(F_{U\text{-}O})/14.103$. The constant calculated for the $[UO_2(C_4H_3N_2O_5)_2].4H_2O$ complex is found to be 8.01 mdyn/A°. This value was then substituted into Jones relation [34, 35]: $R_{U\text{-}O} = 1.08(F_{U\text{-}O})^{-1/3} + 1.17$. The values of $R_{U\text{-}O}$ are found = 1.71 for the uranyl(II) complex. The calculated value of $F_{U\text{-}O}$ is fall in the usual range for the uranyl complexes [34, 35]. On the other hand, concerning, the infrared spectra of $[ZrO]^{2+}$ complex show a medium absorption band at 1071 cm^{-1} due to ν(Zr=O) as expected [32, 32]. The ν(V=O) band is appeared at 845 cm^{-1} [31, 32]. The bands assigned for ν(M-O) and ν(M-N) are appeared at low frequency region 500-600 cm^{-1} for all isolated complexes. The appearance of band assigned to ν(OH) as well as the little broadness appeared supporting the presence of water of crystallization attached physically with the complex sphere. So that, each ligand coordinates as mononegative bidentate mode towards the center metal ions. The bands appeared at ~ 800 and 700 cm^{-1} in Sn(II), UO(II), VO(II), and ZrO(II) complexes are referring to δ_r and δ_w water molecules.

Table 2. FTIR frequencies (cm^{-1}) of alloxan and their Sn(II), UO(II), VO(II), and ZrO(II) alloxante complexes.

Compound	ν (OH)+ ν(NH)	νC(4)=O + νC(6)=O	ν(N=C-O)
Alloxan	3339-3044	1726	-
I	3354-2854	1713	1642
II	3415	1710	1640
III	3420	1712	1638
IV	3359-2924	1711	1642

[*]Alloxan = ν(C(2)=O) at 1764 cm^{-1} and ν(C(5)=O) at 1737 cm^{-1}.

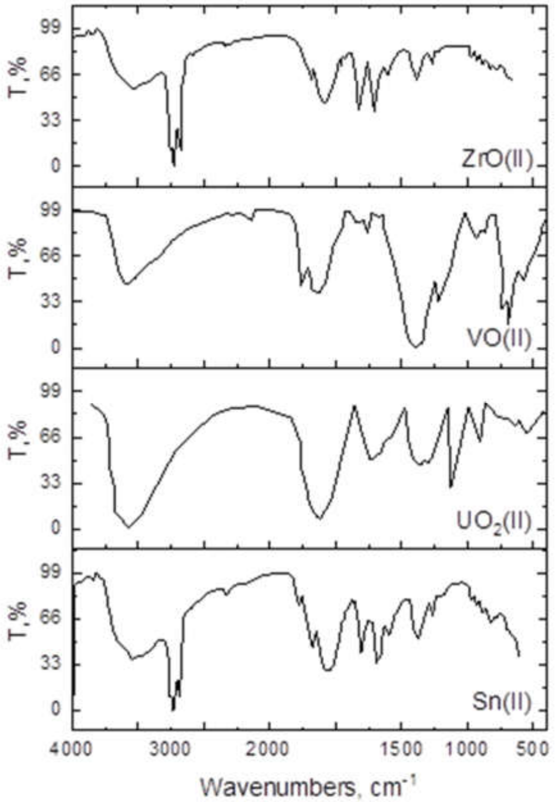

Figure 4. FTIR spectra of Sn(II), UO(II), VO(II), and ZrO(II) alloxan complexes.

Electronic spectra

The UV-Vis spectra of the alloxan ligand and their tin(II), uranyl(II), vanadyl(II) and zirconyl(II) alloxanate complexes are scanned. The electronic spectra are measured in 10^{-3} M DMSO. The ligand spectra showed the expected π→π* transition at the region 200-265 nm. The electronic spectra of $[Sn(C_4H_3N_2O_5)_2].10H_2O$ and $[ZrO(C_4H_3N_2O_5)_2].8H_2O$ complexes have some spectral bands at (225, 245 and 260 nm) and (220, 245 and 265 nm) attributed to the π→π* and $L–M_{CT}$ transitions. The electronic spectrum of the vanadyl complex $[VO(C_4H_3N_2O_5)_2].6H_2O$ exhibits bands at (220 and 230 nm), 310 nm, 500 nm, and 745 nm which can be assigned to the π→π* transition of the alloxan ring, intraligand charge transfer band (INCT), $^2B_2(P)\rightarrow E$ and $^2B_2\rightarrow{}^1A_1$ transitions, respectively. These transition, as well as the measured value of magnetic moment (1.3 B.M.) suggest square pyramidal stereochemistry of the vanadyl(II) complex. These results are in excellent agreement with those achieved earlier [36]. Since uranyl complexes contain U(VI) with an empty valence shell, the metal center is only capable to function as an acceptor moiety for LMCT transition. It seems that the charge transfer band (LMCT) from oxide (=O) to uranyl occurred at lower frequencies (higher wavelengths) than the alloxan→U(VI) [37]. The magnetic moment values, μ_{eff}, measured for all complexes at room temperature and recorded in the solid state. The Sn(II), UO(II), and ZrO(II) alloxan complexes showed diamagnetic values for magnetic and electronic measurements.

^{1}H NMR spectra

The ^{1}H-NMR spectrum of the free alloxan ligand, there are four peaks, the peaks appearing at 11.23 and 2.25 ppm can be attributed to N-H and O-H in the lactam form, respectively. The peak at 7.47 ppm can be attributed to N-H in position 3 when the alloxan converted to monoenol I form, confirming the different tautomeric forms of alloxan. The fourth peak at 3.26 ppm is due to the presence of water of hydration. The spectrum of ZrO(II) complex is different from the spectrum of the free ligand. The spectrum of the [ZrO($C_4H_3N_2O_5$)$_2$] complex contain four peaks. The first peak at 10.30 ppm, can be attributed to N-H in position 3 (monoenol I form). The second peak at 8.00 ppm can be attributed to N-H in position 1 (monoenol II form), the proton in N-H in position 1 had transferred to the oxygen in position 2. The third one at 3.25 ppm is due to the presence of water of hydration. The fourth at 2.55 may be attributed to hydroxyl group. The presence of these peaks confirms that the chelating ring in this type of complex (Type 1) is through the nitrogen in position 1 and deprotonated of hydroxyl group in position 2.

Thermogravimetric analysis

Thermal analysis curves (TG and DTG) for the studies alloxanate complexes are shown in Figure 5. The results of the thermal analysis are summarized in Table 3. Thermal decomposition of alloxan complexes occurs in two to four steps. The first and second decomposition steps related to the Sn(II), UO(II), VO(II), and ZrO(II) alloxan complexes are dedicated to releasing nH_2O molecules out of the coordination sphere. From the second to last decomposition steps dealing with the loss of organic resting (the alloxan molecules) see Table 3. The final residues at the end of the decomposition processes in all solid isolated complexes were assigned to the metal oxides contaminated with few carbon unoxidized atoms.

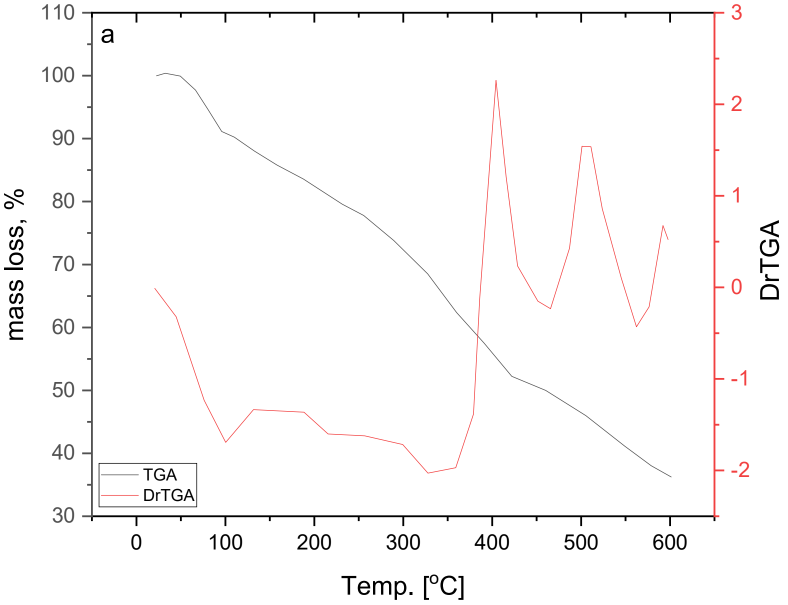

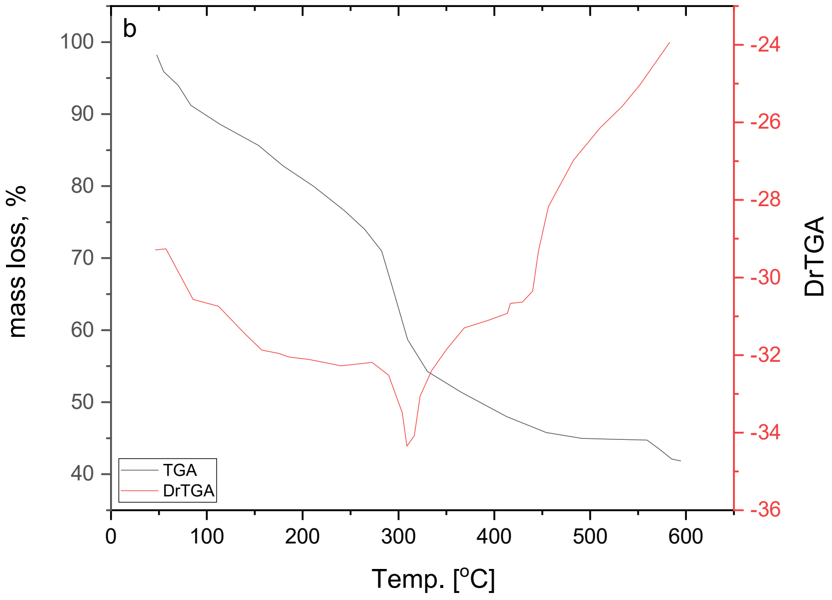
b
mass loss, %
100
90
80
70
60
50
40
DrTGA
-24
-26
-28
-30
-32
-34
-36
0
100
200
300
400
500
600
Temp. [oC]
TGA
DrTGA

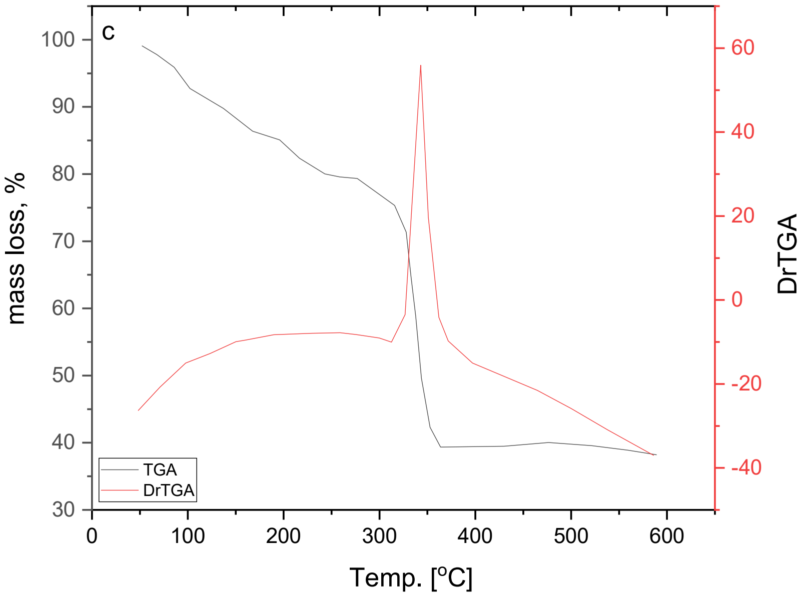
c
mass loss, %
100
90
80
70
60
50
40
30
DrTGA
60
40
20
0
-20
-40
0
100
200
300
400
500
600
Temp. [oC]
TGA
DrTGA

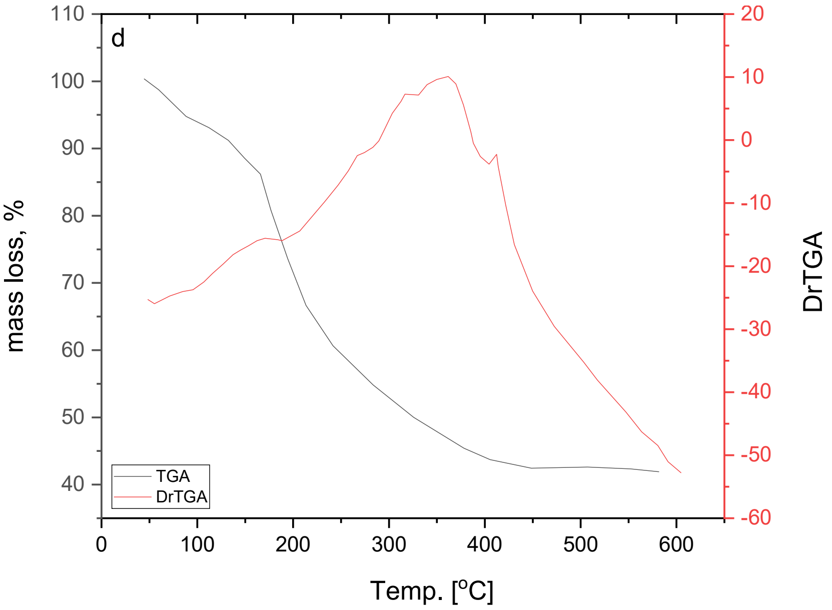

Figure 5. TGA curves of (a) Sn(II), (b) UO(II), (c) VO(II), and (d) ZrO(II) alloxan complexes.

Table 3. Thermogravimetric results of the alloxanate complexes.

Complexes	Steps	Temperature range (°C)	DTG peak (°C)		TG Weight loss (%)		Assignments
			Endo	Exo	Calc.	Found	
Sn(II)	1st	30-150	100	-	11.67	11.50	$4H_2O$
	2nd	150-350	328	-	17.50	17.20	$6H_2O$
	3rd	350-480	-	466	17.37	17.60	Dec. Alloxan molecule
	4th	480-800	-	562	17.37	17.50	Dec. Alloxan molecule
	residue				36.09	36.20	SnO2 + 6C
UO_2(II)	1st	30-100	87	-	10.91	11.00	$4H_2O$
	2nd	105-200	160	-	25.91	25.90	Dec. Alloxan molecule
	3rd	200-800	308	-	22.27	22.10	Dec. Alloxan molecule
	residue				40.91	41.00	UO_2
VO(II)	1st	30-180	170	-	21.91	21.80	$6H_2O$
	2nd	180-800	-	340	59.63	60.06	Dec. Alloxan molecule
	residue				18.46	18.14	½V_2O_5
ZrO(II)	1st	30-190	-	167	25.31	25.50	$8H_2O$
	2nd	150-800	-	360	53.03	53.10	Dec. Alloxan molecule
	residue				21.66	21.40	ZrO_2

Kinetic studies

The characteristic parameters of thermal stability were obtained from the analysis of thermometers (Figure 5), which are listed in Table 4. Kinetic parameters such as activation energy (E*) were calculated from Arrhenius plots between decomposition rate (ln K) and 1/T. Decomposition rate measured from the slopes of TGA curves at decomposition temperature. The thermodynamic parameters of the activated complexes, including free energy G*, enthalpy ΔH* and entropy ΔS* of the process were calculated using the Coats and Redfern [38] and the approximation method of Horowitz and Metzger equation [39]. The thermodynamic parameters of the activated complexes are often calculated using the peak temperature T_s (maximum differential thermogravimetric peak) so that the value of ΔG*, H* and S* correlates with the highest rate of the process.

Table 4. Kinetic thermodynamic parameters of alloxanate complexes.

Complex	Method	Parameter					r
		E (kJ mol^{-1})	A (s^{-1})	ΔS (J mol^{-1} K^{-1})	ΔH (kJ mol^{-1})	ΔG (kJ mol$^{-1)}$	
Sn(II)	CR	2.10×10^4	5.87×10^6	-1.06×10^2	1.50×10^4	9.22×10^4	0.9734
	HM	2.88×10^4	1.10×10^6	-1.58×10^2	2.70×10^4	8.89×10^5	0.9982
UO_2(II)	CR	1.66×10^5	1.45×10^{13}	-1.44×10^2	1.65×10^5	1.62×10^5	0.9958
	HM	1.71×10^5	1.04×10^{15}	-2.15×10^2	1.84×10^5	1.69×10^5	0.9922
VO(II)	CR	4.14×10^4	1.32×10^4	-1.91×10^2	3.65×10^4	1.20×10^5	0.9965
	HM	4.11×10^4	1.30×10^2	-2.00×10^2	3.70×10^4	1.42×10^5	0.9954
ZrO(II)	CR	2.67×10^4	3.22×10^5	-1.49×10^2	2.30×10^4	9.26×10^4	0.9891
	HM	2.55×10^4	1.98×10^2	-2.20×10^2	2.45×10^4	8.50×10^5	0.9983

Negative values of ΔS* indicate that the activated complexes have more ordered structures than the reactant [40]. The enthalpy activation, ΔH^*, and Gibbs free energy, ΔG^*, were calculated from; $\Delta H^* = E^* - RT$ and $\Delta G^* = \Delta H^* - T\Delta S^*$, respectively. ΔG is positive for reaction for which ΔH is positive and ΔS is negative. The reaction for which ΔG is positive and ΔS is negative considered as unfavorable or non-spontaneous reactions. Reactions are classified as either exothermic ($\Delta H < 0$) or endothermic ($\Delta H > 0$) based on whether they give off or absorb heat. Reactions can also be classified as exergonic ($\Delta G < 0$) or endergonic ($\Delta G > 0$) based on whether the free energy of the system decreases or increases during the reaction.

ACKNOWLEDGEMENT

Taif University Researches Supporting Project number (TURSP-2020/01), Taif University, Taif, Saudi Arabia.

REFERENCES

1. Brugnatelli, L. SUR unAcide nouveau obtenu en traitantl'acideuriqueparl'acidenitrique. *Ann. Chim. Phys.* **1818**, 8, 201-206.
2. Holla, B.S.; Rao, B.S.; Sarojini, B.K.; Akberali, P.M. One pot synthesis of thiazolodihydropyrimidinones and evaluation of their anticancer activity. *Eur. J. Med. Chem.* **2004**, 39, 777-783.
3. Bhargava, S.K.; Singh, T.G.; Mannan, A.; Singh, S.; Gupta, S. Pharmacological evaluation of *Thuja occidentalis* for the attenuation of nephropathy in streptozotocin-induced diabetes rats. *Obes. Med.* **2022**, 31, 100391.
4. Lartey, N.L.; Asare-Anane, H.; Ofori, E.K.; Antwi, S.; Asiedu-Larbi, J.; Ayertey, F.; Okine, L.K.N. Antidiabetic activity of aqueous stem bark extract of *Annickia polycarpa* in alloxan-induced diabetic mice. *J. Tradit. Complement. Med.*, **2021**, 11, 109-116.
5. Maxwell, K.G.; Millman, J.R. Applications of iPSC-derived beta cells from patients with diabetes. *Cell Rep. Med.* **2021**, 2, 100238.

6. Jain, K.; Logothetopoulos, J. Proinsulin biosynthesis by pancreatic islets of the rat and the study of alloxan cytotoxicity in vitro. *Biochim. Biophys. Acta* **1976**, 435, 145-151.
7. Yamamoto, H.; Uchigata, Y.; Okamoto, H. Streptozotocin and alloxan induce DNA strand breaks and poly(ADP–ribose) synthetase in pancreatic islets. *Nature* **1981**, 294, 284-286.
8. Uchigata, Y.; Yamamoto, H.; Kawamura, A.; Okamoto, H. Protection by superoxide dismutase, catalase, and poly(ADP-ribose) synthetase inhibitors against alloxan- and streptozotocin-induced islet DNA strand breaks and against the inhibition of proinsulin synthesis. *J. Biol. Chem.* **1982**, 257, 6084-6088.
9. Yamamoto, H.; Uchigata, Y.; Okamoto, H. DNA strand breaks in pancreatic islets by in vivo administration of alloxan or streptozotocin. *Biochem. Biophys. Res. Commun.* **1981**, 103, 1014-1020.
10. Bojarski, J.T.; Mokrosz, J.L.; Paluchowska, M.N. Recent progress in barbituric acid chemistry. *Adv. Heterocycl. Chem.* **1985**, 38, 229-297.
11. Wakefield, B.J. in *Comprehensive Organic Chemistry*, Vol. 3, Barton, D.H.R.; Ollis, W.D. (Eds.), Pergamon Press: Oxford; **1979**; p. 943.
12. Lange, W.E.; Foyc, W.O. Metal chelates of alloxan. *J. Am. Pharm. Ass.* **1956**, 45, 699-701.
13. Refat, M.S.; El-Korashy, S.; Kumar, D.N.; Shahat, A. Spectral and thermal studies of alloxan complexes. *J. Coord. Chem.* **2008**, 61, 1935-1950.
14. Saxena, M.C.; Bhattacharya, A.K. Complex formation between trivalent cerium and alloxan. *Z. Anorg. Allg. Chem.* **1962**, 315, 114-117.
15. Shebaldina, L.S., Kovalchukova, O.V., Strashnova, S.B.; Zaitsev, B.E.; Ivanova, T.M. Synthesis and physicochemical properties of d- and f-metal complexes with alloxan. *Russ. J. Coord. Chem.* **2004**, 30, 38-42.
16. Kakkar, R.; Bhandari, M.; Gaba, R. DFT study of some trivalent d- and f-block metal ion complexes of alloxan. *J. Theor. Comput. Chem.* **2013**, 12, 1350052.
17. Kakkar, R.; Sarma, B.K.; Katoch, V. Theoretical study of the mechanism of proton transfer in tautomeric systems: Alloxan. *J. Chem. Sci.* **2001**, 113, 297-306.
18. Daul, C.; Deiss, E.; Gex, J.N.; Perret, D.; Schaller, D.; Von Zelewsky, A. Alterdentate ligands: Determination of the energy barrier for intramolecular metal ion exchange in complexes of ninhydrin and alloxan radical ions with zinc(2+), magnesium(2+), cadmium(2+), and yttrium(3+). *J. Am. Chem. Soc.* **1983**, 105, 7556-7563.
19. Kovalchukova, O.V.; Gridasova, R.K.; Zaitsev, B.E. Synthesis and the structure of alloxan complex with cobalt(III). *Zh. Neorg. Khim.* **1981**, 26, 985-989.
20. Mordovina, N.I.; Kovalchukova, O.V.; Zaitsev, B.E.; Strashnova, S.B.; Leon Palomino, M.I.; Bel'skii, V.K.; Stash, A.I.; Nikitin, S.V.; Ryabov, M.A. Complexes of d and f metals with 2-methyl-3-hydroxy(amino)pyrido[1,2-a]pyrimidine-4-one. Crystal structure of 2-methyl-3-hydroxypyrido[1,2-a]pyrimidine-4-one. *Russ. J. Coord. Chem.* **2003**, 29, 880-885.
21. Kovalchukova, O.V.; Molodkin, A.K.; Gridasova, R.K. Synthesis of cobalt(II) and nickel(II) compounds with some barbituric-acid derivatives. *Zh. Neorg. Khim.* **1983**, 28, 1067-1071.
22. Masoud, M.S.; Mohamed, R.H.A.; Kamel, H.M.; El-Ziani, N.O.M. Solvent effect effects on the electronic absorption spectra of some an analytical indicator. *BAU J. – Sci. Technol.* **2020**, 1, 1-11.
23. Gupta, R.; Saxena, R.K.; Chatarvedi, P.; Virdi, J.S. Chitinase production by streptomyces viridificans: Its potential in fungal cell wall lysis. *J. Appl. Bacteriol.* **1995**, 78, 378-383.
24. von Zelewsky, A. Alterdentate ligands. *Inorg. Chem.* **1981**, 20, 4448-4449.
25. Bolton, W. The crystal structure of alloxan. *Acta Cryst.* **1964**, 17, 147-152.
26. Swaminathan, S.; Craven, B.M.; McMullan, R.K. Alloxan - electrostatic properties of an unusual structure from X-ray and neutron diffraction. *Acta Cryst.* B **1985**, 41, 113-122,
27. Mootz, D.; Jeffrey, G.A. The crystal structure of 5,5-dihydroxybarbituric acid trihydrate. *Acta Cryst.* **1965**, 19, 717-725.

28. Singh, C. The structure of the pyrimidines and purines. VIII. The crystal structure of alloxan $C_4H_4N_2O_5$. *Acta Cryst.* **1965**, 19, 759-767.
29. Allehyani, B.H.; Elroby, S.A.; Aziz, S.G.; Hilal, R.H. Protonation and deprotonation enthalpies of alloxan and implications for the structure and energy of its complexes with water: a computational study, *J. Biomol. Struct. Dyn.* **2015**, 33, 897-910.
30. Palomino, L.; Yvette, M.; Gridasova, R.K.; Zaitsev, B.E.; Kovalchukova, O.V. Synthesis and structure of an iron (III) complex with alloxane. *Zh. Neorg. Khim.* **1987**, 32, 2583-2586.
31. Refat, M.S. Complexes of uranyl(II), vanadyl(II) and zirconyl(II) with orotic acid “vitamin B13”: Synthesis, spectroscopic, thermal studies and antibacterial activity. *J. Mol. Struc.* **2007**, 842, 24-37.
32. Nakamoto, K. *Infrared and Raman Spectra of inorganic and coordination compounds*, 3rd ed., Wiley Interscience: New York; **1978**.
33. El-sonbati, A.Z.; Diab, M.A.; El-Asmy, A.A. Uranium(VI) complexes of some Schiff bases derived from hydroxyaromatic aldehyde and ketone. *Synth. React. Inorg. Met.-Org. Chem.* **1989**, 19, 731-740.
34. Mello, L.S.; Cruz, Jr, J.W.; Bucalon, D.H.; Romera, S.; Santos, M.P.; Liao, L.M.; Vizotto, L.; Martins, F.T.; Dockal, E.R. Synthesis, characterization and crystal structure of racemic vanadyl and uranyl salen-type complexes. *J. Mol. Struc.* **2021**, 1228, 129656.
35. Faheim, A.A.; Elsawy, M.M.; Salem, S.S.; Abdel El-Wahab, H. Novel antimicrobial paint based on binary and ternary dioxouranium (VI) complexes for surface coating applications. *Prog. Org. Coat.* **2021**, 151, 106027.
36. Adam, M.S.S.; Khalil, A. Nickel(II), copper(II), and vanadyl(II) complexes with tridentate nicotinoyl hydrazone derivative functionalized as effective catalysts for epoxidation processes and as biological reagents. *J. Taiwan Inst. Chem. Eng.* **2022**, 132, 104192.
37. Riisiö, A.; Väisänen, A.; Sillanpää, R. Uranyl complexes of alkyl-bridged ditopic diaminotetraphenol ligands and their use as uranyl ion extractors. *Inorg. Chem.* **2013**, 52, 8591-8600.
38. Coats, A.W.; Redfern, J.P. Kinetic parameters from thermogravimetric data. *Nature*, **1964**, 201, 68-69.
39. Horowitz, H.W.; Metzger, G. A new analysis of thermogravimetric traces. *Anal. Chem.* **1963**, 35, 1464-1468.
40. Wendlandt, W.W. *Thermal Methods of Analysis*, John Wiley and Sons Inc.: New York; **1974**.